

Atae Akhrif<sup>1</sup>,  
Maximilian J. Geiger<sup>2</sup>,  
Marcel Romanos<sup>1</sup>,  
Katharina Domschke<sup>2,3</sup>,  
Susanne Neufang<sup>1\*</sup>

<sup>1</sup>Center of Mental Health, Department of Child and Adolescent Psychiatry, Psychosomatics and Psychotherapy, University of Wuerzburg, Wuerzburg, Germany

<sup>2</sup>Center of Mental Health, Department of Psychiatry, Psychosomatics and Psychotherapy, University of Wuerzburg, Wuerzburg, Germany

<sup>3</sup>Department of Psychiatry and Psychotherapy, University of Freiburg, Hauptstrasse 5, D-79104 Freiburg, Germany

Received 18 March 2017  
accepted 5 September 2017

## 1. Introduction

In recent years, translational studies comparing imaging data of animals and humans have gained increasing scientific interests with crucial findings stemming from both human and animal works. In order to harmonize statistical analysis of data from different species and to optimize the transfer of knowledge between them, shared data acquisition protocols and/or combined statistical approaches have to be identified. Following this idea, we applied a statistical approach, which has until now mainly been used to model neural responses of electrophysiological recordings from rodent data, on human hemodynamic responses (i.e. Blood-Oxygen-Level-Dependent BOLD signal) as measured via fMRI. The statistical approach is Bayesian Adaptive Regression Splines (BARS). BARS is a smoothing algorithm/curve fitting technique. In neuroscience it is used to smooth neural time courses, spike trains and tuning curves from neurophysiological recordings

# TASK PERFORMANCE CHANGES THE AMPLITUDE AND TIMING OF THE BOLD SIGNAL

## Abstract

Translational studies comparing imaging data of animals and humans have gained increasing scientific interests. With this upcoming translational approach, however, identifying harmonized statistical analysis as well as shared data acquisition protocols and/or combined statistical approaches is necessary. Following this idea, we applied Bayesian Adaptive Regression Splines (BARS), which have until now mainly been used to model neural responses of electrophysiological recordings from rodent data, on human hemodynamic responses as measured via fMRI. Forty-seven healthy subjects were investigated while performing the Attention Network Task in the MRI scanner. Fluctuations in the amplitude and timing of the BOLD response were determined and validated externally with brain activation using GLM and also ecologically with the influence of task performance (i.e. good vs. bad performers). In terms of brain activation, bad performers presented reduced activation bilaterally in the parietal lobules, right prefrontal cortex (PFC) and striatum. This was accompanied by an enhanced left PFC recruitment. With regard to the amplitude of the BOLD-signal, bad performers showed enhanced values in the left PFC. In addition, in the regions of reduced activation such as the parietal and striatal regions, the temporal dynamics were higher in bad performers. Based on the relation between BOLD response and neural firing with the amplitude of the BOLD signal reflecting gamma power and timing dynamics beta power, we argue that in bad performers, an enhanced left PFC recruitment hints towards an enhanced functioning of gamma-band activity in a compensatory manner. This was accompanied by reduced parieto-striatal activity, associated with increased and potentially conflicting beta-band activity.

## Keywords

Functional Neuroimaging • Bayesian Adaptive Regression Spline • fMRI time courses • attention


[1-3], as well as regional fMRI time courses [4]. The graphical data representation of peristimulus-time histograms (PSTH) of a data set, for example spike trains of a single neuron is accumulated for all trials under a particular set of experimental conditions to show the firing rate varies over time. One reason the PSTH works well is that our eye is able to smooth the PSTH so that we see the temporal evolution of the firing rate. However, once we have articulated the goal of estimating the firing rate, it is possible to improve the PSTH by smoothing [5]. Estimating the firing rate in this context means producing an estimate of the instantaneous firing rate, which we write as  $\lambda(t)$ , at each time  $t$ , where  $t$  varies across a whole range of experimental values of interest. In other words, we are interested in estimating the curve described by  $\lambda(t)$  [5]. BARS uses cubic splines (piecewise cubic polynomials) which are joined at selected points called 'knots' [4,6], with the number of knots and their locations being based on a posterior probability

distribution. The expectation of the unknown function of time is then taken to be the fitted curve [2,5,7-9].

In our study, BARS describes the fluctuations of the amplitude of the BOLD signal over the course of the entire measurement. The resulting curve is described by estimating the expectation value of a certain event (e.g. neural firing, increase of the amplitude of the BOLD signal), which is written as  $\lambda$  at each time point  $t$  ( $\lambda(t)$ ) and its fluctuation over the time course in terms of peaks and valleys.

The relation between electrophysiological recordings and BOLD response has been empirically proven by Logothetis and coworkers in numerous studies. They have found that local field potentials (LFPs) reflect the best hemodynamic responses and it is mainly the component of the gamma band (60–120 Hz) which correlated positively with fMRI data [10]. Subsequent studies were able to differentiate between amplitude and timing characteristics the way the amplitude

\* E-mail: Neufang\_S@ukw.de

 © 2017 Atae Akhrif et al., published by De Gruyter Open.

This work is licensed under the Creative Commons Attribution-NonCommercial-NoDerivs 3.0 License.

of the BOLD signal reliably reflected both the increases and decreases in gamma power. Timing dynamics of the BOLD signal, in turn, reflect activity in the beta band (18-28 Hz) [11], with a higher beta power corresponds to faster increases (slower decreases) of the BOLD signal, and reciprocally a lower beta power to faster decreases (slower increases) of the BOLD signal. In the cognitive domain, neural oscillations in the gamma frequency band play a crucial role in the synchronization of neural firing as well as in conscious cognitive information processing and focused attention [12]. On the other hand, beta band oscillations have been associated with selective attention [e.g. 13], where a decrease of activity reflects a state of increased processing capabilities [14]. In order to prove that BARS when applied on fMRI time series corresponds to neural processing like it does on neurophysiological recordings, we have additionally performed: i) conventional analyses of brain activation patterns using GLM in terms of an external validation and, ii) task performance of an attention task which the volunteers had to perform in the MRI scanner for behavioral correlate/ecological validation.

The present sample of healthy volunteers underwent a task-fMRI measurement using the Attentional Network Task (ANT) by Fan et al. (2005) [15]. The ANT has been used in numerous fMRI as well as EEG-studies to show most robust responses in the fronto-parietal regions as well as the striatum in terms of increased brain activation [16,17], as well as reflected by the event-related potential P300 in parietally-located electrodes [e.g. 18]. In addition, behavioral attention network scores significant correlation of the beta and gamma powers in the fronto-central regions [19]. Within a fronto-parieto-striatal attention network, the fronto-striatal loop has been associated with inhibiting response of the prefrontal cortex (PFC) representing a top-down control, which means the ability to focus on the current task and not being distracted by further stimulations [20], and the striatum being responsible for motor and impulse control. The parietal lobe (PL), in turn, is understood as a bottom-up structure, perceiving task-relevant and irrelevant stimuli and then reporting these perceptions to higher-order cortical structures such as the PFC.

Within the fronto-parieto-striatal attention network, brain activation patterns and  $\lambda(t)$  were determined. Task performance was operationalized by splitting the subjects into groups of good and bad performers according to their overall accuracy. Group differences were addressed in the behavioral data, brain activation maps and expectation values  $\lambda(t)$ . We expected to differentiate good performers from bad performers: (a) based on the behavioral level with a significantly higher overall accuracy (the grouping criteria), and (b) brain activation with a stronger frontal top-down control reflected by higher activation in the fronto-striatal regions. With regard to the relation between brain activation and BARS, we expected to find that (c) regions with a higher brain activation would also present higher expectation values, reflecting a higher gamma power. On the other hand, regions of reduced brain activation were supposed to go along with stronger fluctuating expectation values  $\lambda(t)$ , indicating stronger beta power.

## 2. Materials And Methods

### 2.1 Subjects

Forty-seven participants ( $f=23$ ,  $m=24$ ; mean age:  $25.43 \pm 2.7$  years) were examined in the present fMRI study. This sample has previously been investigated for the genetic influence of brain activation patterns of alerting and executive attention using GLM [16,21]. Subjects were drawn from a large pool of healthy German subjects consecutively recruited at the Department of Psychiatry, University of Wuerzburg, Germany. All subjects were screened for the absence of current or life-time history of mental axis I disorders by experienced clinical psychologists or psychiatrists using the Mini International Neuropsychiatric Interview (MINI) [22]. Right-handedness was ascertained using the Edinburgh Handedness Inventory [EHI; 23]. The study was approved by the ethics committee of the Faculty of Medicine, University of Wuerzburg, Germany, and was conducted in accordance with the declaration of Helsinki in its latest version from 2008. Written informed consent was obtained from all subjects.

### 2.2 Paradigm

The used paradigm was the ANT as described in Fan et al. 2005. The ANT requires the participants to determine whether the central arrow out of 5 horizontally-arranged arrows pointing left or right. Each trial consisted of five events. First, there was a 400 ms fixation period, followed by a 150 ms warning cue. There was either a non-spatially informative double cue, a spatial cue, or alternatively, no cue was presented. After a cue-target interval of 400 ms, a target was presented for 1050 ms, consisting of the target arrow and 4 context flankers.

In order to ensure a variation between stimulus onset and image acquisition, null events were randomly presented in the course of the task. Null events did not represent an experimental condition and thus were not included into the statistical model. Out of 256 trials, there were 64 target events preceded by a double cue, 64 events preceded by a spatially informative cue, 64 events without a cue and 64 null events. In 50% of the experimental trials, targets were congruent (96 trials) and another 50% for incongruent. Trials were presented in a randomized order across all subjects. Total trial duration for null events was 2000 ms, target events were 3000 ms long. Overall, the completion of the task took 14 minutes.

### 2.3 Data Acquisition

fMRI data was acquired on a 3 Tesla TRIO scanner (Siemens, Erlangen, Germany). Whole-brain T2\*-weighted BOLD images were recorded with a gradient echo isotropic  $3 \times 3 \times 3 \text{ mm}^3$  EPI sequence (repetition time  $TR=2000$  ms, echo time  $TE=30$  ms, 36 slices, 3 mm slice thickness, field of view  $FoV=192$  mm, flip angle  $=90^\circ$ , 420 volumes). In addition, anatomical images were obtained from each subject using a T1-weighted MPRAGE (Magnetization Prepared Rapid Gradient Echo) with the sequence parameters  $TR=2.3$  s,  $TE=2.95$  ms, 176 slices, 1 mm slice thickness,  $FoV=270$  mm, flip angle  $=9^\circ$ ).

### 2.4 Behavioral Data Processing and Statistical Analysis

Accuracy was defined as the proportion of correct trials from all trials, reaction time was calculated between target presentation

and response. On the behavioural level, the efficiency of three different attentional networks, namely the alerting, orienting and executive attention system was assessed by measuring how response times were influenced by cues without spatial information (alerting), spatial cues indicating the position of the target position (orienting), and congruent and incongruent flankers (executive attention):  

$$\text{alerting} = \text{rt}_{\text{no cue}} - \text{rt}_{\text{double cue}}$$

$$\text{orienting} = \text{rt}_{\text{double cue}} - \text{rt}_{\text{spatial cue}}$$

$$\text{and executive attention} = \text{rt}_{\text{incongruent targets}} - \text{rt}_{\text{congruent targets}}$$
 Performance-based differences were revealed using a two sample t-test with the performance group as a group factor and behavioral parameters as dependent variables. Results were significant when they passed a threshold of  $p < .05$ , FDR-corrected for five comparisons.

## 2.5 fMRI-Data Preprocessing

fMRI data was pre-processed and analysed with SPM12 (Wellcome Trust Centre for Neuroimaging London, UK). During pre-processing, all functional images were realigned to the first functional volume for movement correction, unwarped as a correction of field inhomogeneities, spatially normalized into a standard stereotactic space (Montreal Neurological Institute, MNI), resampled to isotropic  $2 \times 2 \times 2 \text{ mm}^3$  voxel and spatially smoothed with a Gaussian kernel of 8 mm full width at half maximum (FWHM). Pre-processing did not include high-pass filtering or global mean correction.

The resulting images entered in both analyses, GLM and BARS, in different formats; whereas whole-brain images (sw\*.nii) entered GLM-based analyses, region-specific time courses were extracted from pre-processed images (for selection of regions see 2.7).

## 2.6 GLM: Statistical Analysis

On a single subject level, GLM analysis was performed as follows: onset regressors of the five experimental conditions 'double cue', 'spatial cue', 'no cue', 'congruent target' and 'incongruent target' were implemented as regressors of interest within the statistical model. Onsets of the cue conditions 'double cue' and 'spatial cue' were defined as the time point when a cue was presented, onsets of

the 'no cue conditions' were determined as 550 ms before target presentation (150 ms cue presentation, 400 ms cue-target interval). Onsets of target conditions were defined as the onset of target presentation. Only correct trials entered statistical analyses, onsets of error trials and six movement parameters from realignment, respectively, were added in terms of regressors of no interest. As basis set the canonical hemodynamic response function was chosen, model derivatives were not used. Data was high-pass filtered with a default size of 120s to reduce data from physiological noise such as breathing, heart rate etc.

On the group level, we aimed to identify these regions, which were activated by the task, i.e. the Main Effect of the Attention Network Task defined as 'double cue' + 'spatial cue' + 'no cue' + 'congruent target' + 'incongruent target' > implicit baseline (contrast weights: 1 1 1 1 1). We analysed this contrast over all subjects as well as with regard to potential group differences. Therefore, we performed a one-way ANOVA model using the performance group as an independent factor (good vs. bad performers) and activation maps as the dependent variables. Activation was considered significant when  $p < .05$  FDR-corrected for multiple comparisons.

## 2.7 BARS: Expectation value of a BOLD event

In general, BARS is used to address generalized nonparametric regression (curve-fitting) problems by assuming that a function  $f(x)$  is approximated by cubic splines. The latter is piecewise cubic polynomials, which are joined at locations called 'knots'. A Bayesian Monte Carlo method searches through the space of possible numbers of knots and their locations and provides an optimally fitted curve. The resulting curve is a data-driven estimate of the expectation value of a certain event (e.g. neural firing, increase in MRI signal), which is written  $\lambda$  for each time  $t$  [5].

## 2.8 fMRI Time course Extraction

For the extraction of fMRI time course, (i) the underlying data is important (in our case the pre-processed data) as well as (ii) the exact localization of the region (i.e. the coordinates

of the individual global activation maximum on single subject level).

Regions of Interest (ROI) were areas which have been associated with attention processing in earlier studies (see introduction), namely the prefrontal, parietal and striatal regions. For the identification of global activation maxima for each subject, the contrast Main Effect of the Attention Network Task was defined on a single subject level and the local maxima of each ROI were identified.

Time course extraction was performed on the pre-processed data. Coordinates were then used as the centre of 10mm spheres using MarsBar [24]. Thus, five ROIs (cf. Table 1) were built as the basis of time course extraction for each subject. Following the routine suggested by Brett et al. (2002) (see MarsBar manual, <http://marsbar.sourceforge.net/marsbar.pdf>), time courses of raw fMRI data were extracted (i.e. smoothed files resulting from the pre-processing procedure) [24].

## 2.9 BOLD event definition

As the amplitude of the BOLD signal correlates with the activity of the neurons located in the specific region where it is extracted, we picked the amplitude value as the event of interest. An event corresponds to a BOLD amplitude that exceeds a certain threshold. Threshold definition in BARS is data-driven [2,4-5] or based on the natural scales as described in the blood pressure study by Muniz-Terrera et al (2016). In order to find the right value for the threshold, 10% of the maximal value of the amplitude was taken and increased stepwisely until a value was found to differentiate the amplitudes between experimental groups. In our case, a thirty per cent of its overall maximum value. In probability theory, stochastic sequences of event times are best modeled using the point processes models. The simplest and most important point process model is the Poisson process. A number of events within a time window, the number of events one would expect to happen during an interval of time, therefore follows the Poisson distributions. In its general form, a point process is modeled by specifying its conditional intensity,  $\lambda(t)$ , which represents the infinitesimal rate at which events are

expected to occur around a particular time  $t$ , conditional on the prior history of the point process prior to time  $t$ . For a non-parametric estimate of  $\lambda(t)$ , we applied BARS to smooth the Peri Event Time Histogram (PETH) of MRI data to get the average ROI response of all subjects.

### 2.10 Raster Plot and PETH

A raster plot marks the occurrence of an event along the X-axis with a tick mark indicating the time it happens (see Fig. 1A). It displays the trial response of a specific ROI. To get the average response of a task, this procedure is repeated several times on a single subject level or over several subjects. An average ROI response

is captured by the PETH showing how the behavior varies across time (see Fig. 1B). For the Y-axis to indicate the conditional intensity, each bin event count is divided by both, the bin width and the number of trials on single subject level/ subjects. The shape of a histogram, or a PETH, changes every time the bin size changes. To get accurate values and comparable results across different trials, it is therefore important to look for an optimal size for the bin. The algorithm we used to calculate the optimal bin size was suggested by Shimazaki and Shimoto, 2007 [25]. The resulting optimal bin number is 60 in our case. In the last step, we used the MATLAB version of the code published by Wallstrom et al. (2008) to smooth the PSTH [26] (see Fig. 1C).

### 2.11 BARS: Statistical Analysis

In order to statistically approach the spline, we determined: (a)  $\lambda_{\text{mean}}$ , i.e. the average expectation value of all bin-specific  $\lambda(t)$ , (b) the range of  $\lambda(\lambda_{\text{range}})$  being the range from the maximum and minimum  $\lambda$  value, and (c) bin-specific  $\lambda(t)$ , group comparisons were statistically addressed using the non-parametric Mann-Whitney Tests with performance group as an independent factor (good vs. bad performers) and  $\lambda_{\text{mean}}, \lambda_{\text{range}}$  as well as bin-specific  $\lambda(t)$  as the dependent variables. Effects were considered significant when passing a statistical threshold of  $p < .05$  FDR-corrected.

The characterisation of the timing was based on the number of peaks and valleys and was reported descriptively.

## 3. Results

### 3.1 Behavioral results

We found that good performers committed less errors (accuracy), responded faster (reaction times) and were not as distracted by incongruent targets as bad performers (executive attention network score). The attention network scores of alerting and orienting we did not differ significantly between groups - (i) accuracy: good performers  $97.9 \pm 1.6\%$ , bad performers  $95.1 \pm 5.2\%$ ,  $T=2.5$ ,  $p < .05$ ; (ii) reaction time: good performers  $504 \pm 57\text{ms}$ , bad performers  $558 \pm 68\text{ms}$ ,  $T=2.9$ ,  $p < .05$ ; (iii) executive attention network: good performers  $55 \pm 13\text{ms}$ , bad performers  $97 \pm 16\text{ms}$ ,  $T=9.5$ ,  $p < .01$ ; (iv) alerting network: good performers  $54 \pm 17\text{ms}$ , bad performers  $51 \pm 24\text{ms}$ ,  $T=0.5$ , n.s.; (v) orienting network: good performers  $77 \pm 26\text{ms}$ , bad performers  $64 \pm 32\text{ms}$ ,  $T=1.4$ , n.s.

### 3.2 GLM results

Across all subjects, we found a significantly activated bilateral fronto-parieto-striatal attention network with significant activation bilaterally within the superior parietal lobe (SPL), middle frontal gyri (MFG) and pallidum (for details see table 1 and Fig. 2), accompanied by an increased activation within the primary motor cortices, reflecting motor activation during button presses ( $x=-56$ ,  $y=-20$ ,  $z=30$ ,  $k=367$ ,  $T=7.1$ ). Only attention-related regions

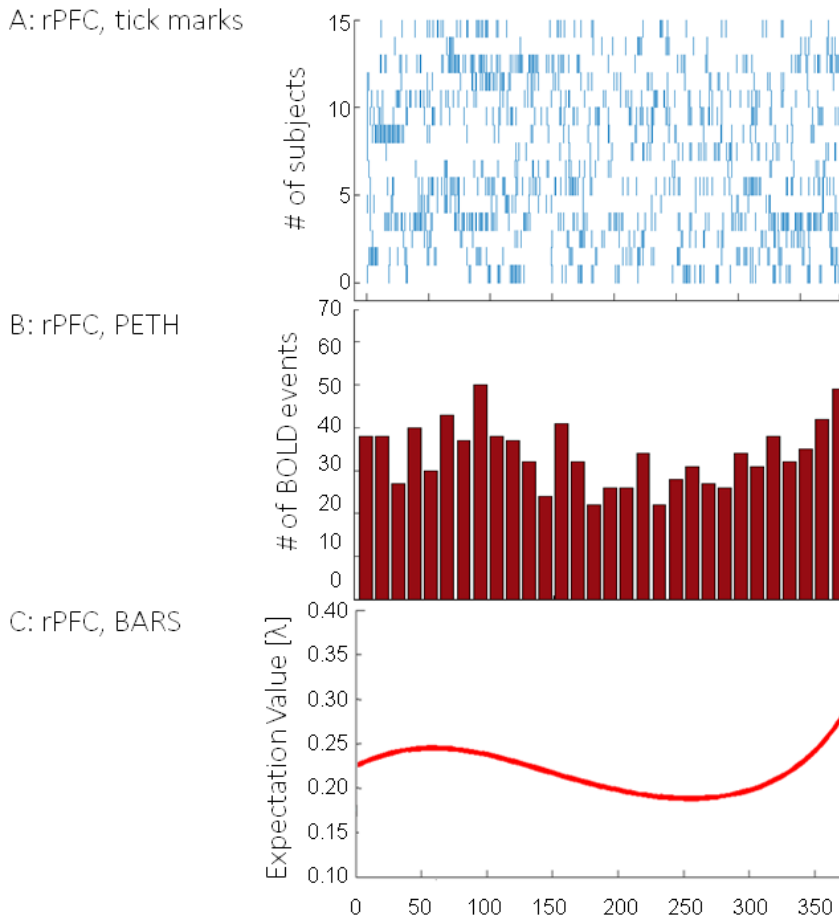


**Fig. 1.** Analysis Steps. Figure 1 represents the analysis steps exemplarily for the task-related time course of the right prefrontal cortex (PFC). In (A), tick marks represent BOLD events of a specific subject (y-axis) at a certain time point (x-axis). In (B), tick marks have been converted into a Peri Event Time Histogram (PETH) by counting the overall number of BOLD events (y-axis) at a certain time bin (x-axis); BARS: Bayesian Adaptive Regression Splines. In (C), the smoothed PETH is shown.

were considered as ROIs and processed for BARS analysis.

The group comparison of the Main Effect of Attention Network Task revealed a significantly stronger activation bilaterally in the SPL, right PFC and striatum in good performers as compared to bad performers. In contrast, bad performers activated the left PFC more strongly (see table 1) (figure 3A).

### 3.3 BARS results

Analyses revealed differences between performance groups bilaterally in the parietal regions, left PFC and striatum with regard to both the average expectation value  $\lambda_{mean}$  and range  $\lambda_{range}$ . The  $\lambda_{mean}$  was significantly higher in the left PFC of bad performers as compared to good performers (ISPL:  $M_{good}=0.35\pm0.07$ ,  $M_{bad}=0.40\pm0.09$ ,  $Z=1.9$ , n.s.; rSPL:  $M_{good}=0.36\pm0.10$ ,  $M_{bad}=0.36\pm0.07$ ,  $Z=0.1$ , n.s.; IPFC:  $M_{good}=0.34\pm0.07$ ,  $M_{bad}=0.41\pm0.08$ ,  $Z=3.0$ ,  $p<.05$ ; rPFC:  $M_{good}=0.33\pm0.05$ ,  $M_{bad}=0.34\pm0.05$ ,  $Z=0.5$ , n.s.; striatum:  $M_{good}=0.32\pm0.04$ ,  $M_{bad}=0.37\pm0.09$ ,  $Z=2.2$ , n.s.), whereas they were similar in all other regions between performance groups. However, expectation values varied more strongly in terms of higher  $\lambda_{range}$  in the left SPL and striatal region in bad performers (ISPL:  $Range_{good}=0.53$ ,  $Range_{bad}=0.61$ ,  $Z=3.2$ ,  $p<.05$ ; rSPL:  $Range_{good}=0.58$ ,  $Range_{bad}=0.47$ ,  $Z=4.1$ ,  $p<.01$ ; IPFC:  $Range_{good}=0.50$ ,  $Range_{bad}=0.46$ ,  $Z=1.6$ , n.s.; rPFC:  $Range_{good}=0.42$ ,  $Range_{bad}=0.44$ ,  $Z=1.2$ , n.s.; striatum:  $Range_{good}=0.16$ ,  $Range_{bad}=0.61$ ,  $Z=21.9$ ,  $p<.01$ ) with no significant differences in the PFC region. In the right SPL, the range was higher in good performers as compared to bad performers. Finally, significant differences in bin-specific  $\lambda(t)$  values were found in all regions except for the right PFC, and also in the enhanced  $\lambda(t)$  values of bad performers as compared to good performers (for detail see table 2).

With regard to the timing characteristics, good performers presented a flat U-shaped curve in all regions except for the right SPL. Bad performers, however, presented several fluctuations in the left SPL ( $n_{good}=1$ ,  $n_{bad}=3$ ), striatum ( $n_{good}=1$ ,  $n_{bad}=4$ ), and left PFC ( $n_{good}=1$ ,  $n_{bad}=2$ ) with significant deviations in the expectation value in several bins (for exact

Table 1. Network Regions, results from GLM analyses

Contrast	x,y,z	Z	Region
Main Effect of the ANT	-28 -56 54	7.8	ISPL
	22 -60 62	7.8	rSPL
	-40 10 34	5.2	IPFC
	38 6 32	4.2	rPFC
	-18 -2 6	4.6	pallidum
good > bad performers	-22 -48 74	3.2	ISPL
	34 -42 48	3.0	rSPL
	32 26 36	3.0	rPFC
			pallidum
bad > good performers	-52 34 2	3.1	IPFC

Note. ISPL: left superior parietal lobe, IPFC: left prefrontal cortex, rSPL: right superior parietal lobe, activation was significant when  $p<.05$ , FDR-corrected for multiple comparisons

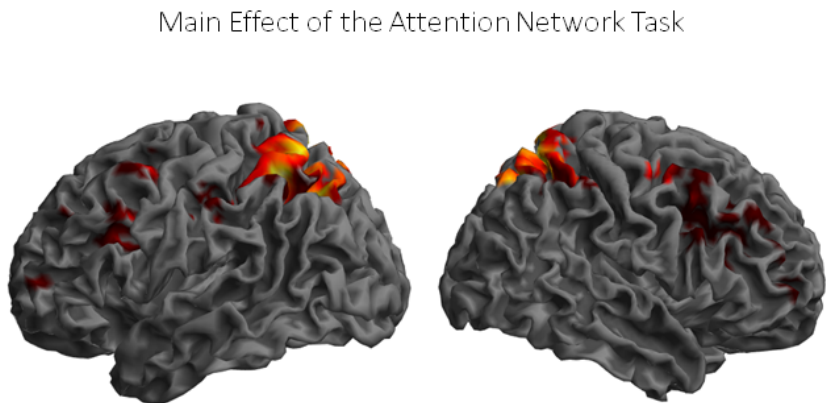


Fig. 2. Brain activation. Figure 2 shows GLM results of the contrast Main effect of the Attention Network Task. The bilateral fronto-parieto-striatal network was significantly activated in  $n=47$ , and  $p<.05$  FWE-corrected.

Table 2. Bin-specific expectation value

Region	Bins	Good performers	Bad performers	Z
ISPL	4-19	.38(.02)	.47(.04)	3.9**
	31-51	.32(.04)	.40(.04)	4.3**
IPFC	37-51	.32(.03)	.37(.03)	3.9**
rSPL	17-44	.25(.01)	.30(.01)	4.0**
striatum	11-28	.24(.004)	.28(.001)	3.4*
	34-54	.32(.01)	.38(.02)	4.2**

Note. ISPL: left superior parietal lobe, IPFC: left prefrontal cortex, rSPL: right superior parietal lobe, \*\*:  $p<.01$ , FDR-corrected for multiple comparisons; \*:  $p<.05$ , FDR-corrected for multiple comparisons.

localization see table 2 and figure 3B). In the right SPL ( $n_{good}=2$ ,  $n_{bad}=2$ ), fluctuations were similar between both groups but were more pronounced in good performers.

### 3.4 Comparing GLM and BARS results

For the last step, we descriptively contrasted results from both analyses, GLM and BARS, to identify convergent and complementary information of both methodological approaches (see table 3). In doing so, we have identified three different patterns in reference



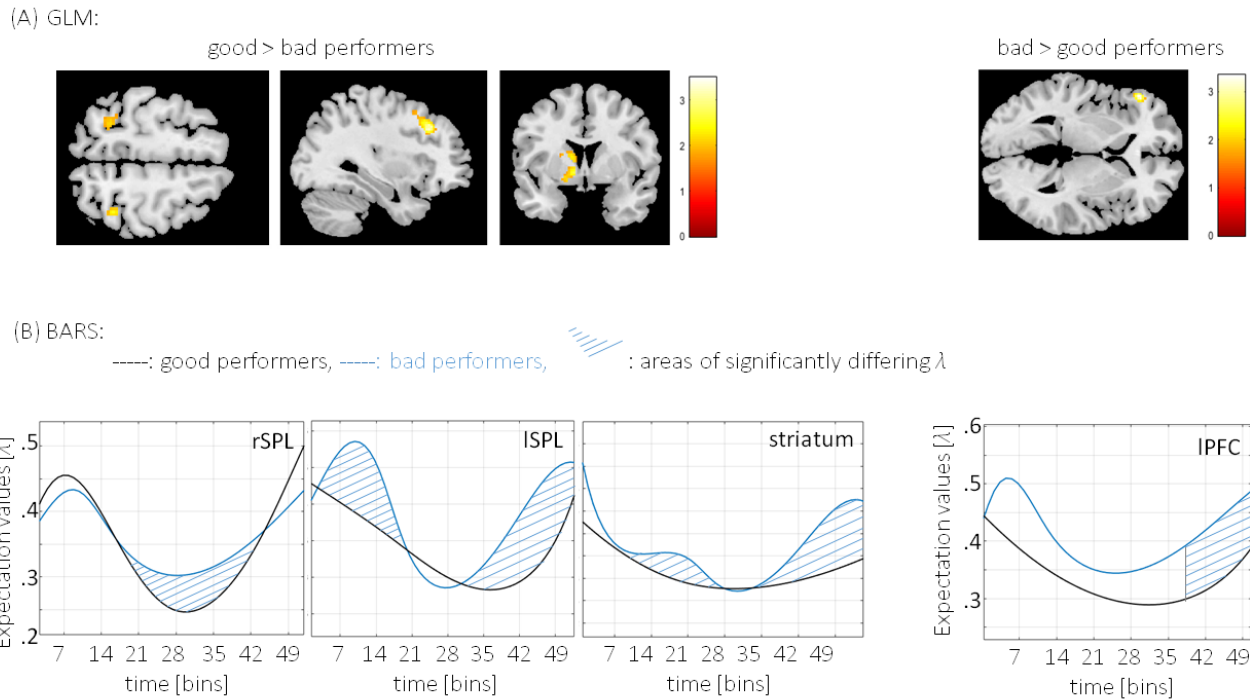


**Fig. 3.** Significant differences in BOLD events in the PFC. In figure 3(A), performance-specific activation patterns are presented: left side- good > bad performers, right side- bad > good performers. Significant activation was overlaid on a standard anatomical brain image. 3(B) shows group-specific BARS for brain regions. The x-axis shows the timeline, indicated by scans, the y-axis represents the expectation value  $\lambda$  for a BOLD event. Blue line - bad performers, black line - good performers, criss-cross lines indicate the bins with significant differing expectation values.

to altered processing in bad performers: (a) stronger activation was combined with an enhanced average expectation values  $\lambda$  and bin-specific  $\lambda(t)$  values in the left PFC, (b) reduced activation was combined with enhanced fluctuation in terms of significantly enhanced range width of the expectation value  $\lambda$  and a higher number of peaks and valleys in the left SPL and striatum. In addition, some of the peaks  $\lambda$  increased significantly, and (c) reduced activation did not show significant differences with regard to  $\lambda$  (e.g. rPFC).

### 4. Discussion

In this study, we have investigated the influence of task performance on multiple levels of attention processing: behavioral performance, brain activation as well as the amplitude and timing of regional time course. We found that bad performers had longer reaction times and higher executive attention network scores on the behavioral level. On the neural level, altered performance was associated with

**Table 3.** Schematic overview of the relation between GLM and BARS parameters highlighting BARS advantage over GLM with regard to timing/beta power information

Region	GLM	$\lambda_{mean}$	$\lambda_{range}$	Timing	$\lambda_{bin-spec}$
(a) enhanced activation & enhanced $\lambda$ in bad performers					
IPFC	↑	↑	n.s.	↑	↑
(b) reduced activation & enhanced fluctuation in bad performers					
ISPL	↓	n.s.	↑	↑	↑
stria	↓	n.s.	↑	↑	↑
(c) similar curvature between performance groups					
rSPL	↓	n.s.	↓	n.s.	↑
rPFC	↓	n.s.	n.s.	n.s.	n.s.

Note. ISPL: left superior parietal lobe, IPFC: left prefrontal cortex, rSPL: right superior parietal lobe

(a) reduced right fronto-striatal and bilateral parietal activation and (b) an enhanced left PFC activation. Additionally, across the entire time course, the left PFC region presented an enhanced BOLD signal amplitude in bad performers, hinting towards a compensatory enhanced gamma power in the left PFC. In the

left SPL and striatum, reduced neural activation was accompanied by an enhanced range width of  $\lambda$  as well as stronger fluctuations during these time courses, suggesting a stronger beta power in bad performers within these regions. Splines in the right SPL and right PFC were similar between performance groups.

#### 4.1 Reduced right fronto-parieto-striatal functioning and enhanced beta power

As introduced, the right frontal and bilateral parietal regions form the core of attention networks [17,27,28], thus the relation between impaired performance and reduced activation in these regions seems plausible. The finding that reduced right fronto-parietal activation was related to an increased beta activity fits nicely into this context, with an increased beta activity hinting towards decreased processing abilities [14]. In detail, bad performers showed higher fluctuations mainly in parietal and striatal processing. Within a fronto-parietal attention network, parietal activity has been associated with bottom-up attentional orienting [29], reflecting screening processes for stimuli [30]. Thus, continuous parietal processing in bad performers might reflect a constant parietal bottom-up processing and indicate a hyperaroused basal attentional state. With regard to beta oscillations in attention processing, firing rates in the pallidum exhibited a linear decrease in sequences of correct responses in a reward learning task in monkeys [31]. In addition, beta oscillations in the human pallidum have been associated with motor control in healthy volunteers [32], as well as with alterations of the same in patients with Parkinson's Disease [33,34]. In sum, a higher beta power in the parietal and striatal regions is associated with altered attentional performance and motor control. In combination with reduced brain activation in the right PFC, reflecting impaired top-down control, our findings revealed a plausible neural explanation for impaired behavioral performance in bad performers.

#### 4.2 Enhanced activation and gamma power in the left PFC

Brain activation as well as gamma activity in the PFC have predominantly been associated with cognitive control, top-down control and attention allocation [35-38]. However, prefrontal recruitment in attentional networks induced by the ANT shows a right-hemispheric preference [15,17], which seems to be ontogenetically determined as developmental studies have reported that a reduction of

left PFC activation with network maturation paralleled with performance improvement [39-41]. Thus, additional activation and increased gamma power in the contralateral PFC might reflect a compensatory mechanism to optimize performance. Alternatively, the left PFC plays a role in attentional processing of verbal learning [42,43], auditory conflict processing [44], and selective attention to lexical and speech sound [45,46]. Thus, it is possible that bad performers in our study used a verbal strategy before or during responding with a button press. A verbal indication of the direction would be mirrored by left PFC activation and gamma power and this might also explain the longer reaction time as verbalization might take some milliseconds.

#### 4.3 The combination of GLM and BARS and the transfer of knowledge between species

In this study, we aimed to prove that BARS applied on human fMRI time courses reflects neural processing as it is the case in the modeling of neural responses of electrophysiological recordings on rodents. We argue that the present combined findings are in line with earlier findings from EEG and fMRI studies as well as from animal and human studies.

However, the application of BARS on fMRI data, to date, has mainly been theoretically in terms of BARS acting as "a flexible denoiser for fMRI time courses, where all smooth sources of variation are combined into the function being estimated", and serving as "a front-end to spatial and regional analyses and group comparisons, automatically incorporating variation in response shape and magnitude across the replicated task blocks in the experiment" [4]. Therefore, this is the first fMRI study empirically applying the BARS approach on fMRI time courses and contrasting it with the standard fMRI data analysis to explore the validity of the approach in cognitive processing, instead of a methodological one. Thus we relied on the theoretical combination of statistical (fluctuations of  $\lambda(t)$  of the BOLD signal) and neuroscientific findings (amplitude and timing of the BOLD signal reflect gamma and beta power). However, to empirically prove the validity of these assumptions, we directly

compare findings from BARS (new approach) with findings from GLM analyses (standard approach) of the same data set as a first dataset specific validation and discuss them in the context of earlier findings in terms of a second external validation. This way we aimed to undermine that BARS is a valid statistical approach to look at characteristics of the BOLD response beyond the usual activation and connectivity patterns.

Nevertheless, it is crucial to gain more experience especially with this approach because BARS addresses brain activation data in terms of curves, not condition-specific activation patterns. To interpret the findings, a change of perspective is needed. For example, Behseta and Chenouri (2011) compared curves of neuronal data between two populations and their reports predominantly consist of the description of differences between groups in curve shapes [3,8]. In our study, we also found that differences were bin-specific, which means they were only significantly different in certain periods of time. For example, gamma power in the left PFC was enhanced in bad performers only in the last quarter of the task. Does this finding reflect a stronger need for concentration in bad performers as compared to good performers at the end of the task based on a higher fatigue in this group? Or is it more likely that this is based on general differences in fluctuations in this region over the course of the whole experiment but significantly only within these bins? To better understand the information provided by BARS from fMRI data, further studies are crucial and needed.

Furthermore, we propose BARS as a potential statistical approach for data analysis across species. In the present human fMRI study, we were not able to directly relate our findings to neurophysiological recordings measuring gamma and beta powers, so the transfer of results relied on literature references and had to be considered theoretically. Therefore, a translational study design would be of high interest, including both neurophysiological recordings from rodents and fMRI time courses from humans acquired while performing the same behavioral paradigm [e.g., 5-choice serial reaction time task; animal version: 47; human version: 48, human fMRI version: 49]. Species-

specific neural data could be analyzed with BARS to extract neural firing/BOLD responses facilitating the direct comparison of findings, and also to improve the interpretation of human results significantly.

Based on the current findings, we conclude that the present results suggest performance variations to be associated with alterations in BOLD amplitude and its temporal dynamics of frontal top-down and bottom-up parietal processing. Based on the relationship between neural signaling and BOLD response, we argue

that bad performance is associated with both increased activation and gamma power in the left PFC, along with a reduced brain activation and an increased beta power in the parietal and striatal areas. With regard to the harmonization of translational study protocols, BARS seems to be a promising tool for data analysis.

### Acknowledgements

This paper was supported by grants from the Interdisciplinary Center for Clinical

Research (IZKF), University of Wuerzburg (N-262 to KD, SN and GH), the Deutsche Forschungsgemeinschaft (DFG; SFB-TRR-58 projects C02 to KD and JD and Z02 to JD and MR) and the Verein zur Durchführung Neurowissenschaftlicher Tagungen e.V. (to SN).

### Conflict Of Interest

No conflicts of interest have been declared.

### References

- [1] Ramezan, R., Marriott P., Chenouri, S., Multiscale analysis of neural spike trains, *Statist. Med.*, 2014, 33, 2, 238-256
- [2] Taubman H., Vaadia E., Paz R., Chechik G., A Bayesian approach for a characterizing direction tuning curves in the supplementary motor area of behaving monkeys, *J. Neurophysiol.*, 2013, 109, 11, 2842-2851
- [3] Behseta S., Chenouri S., Comparison of two populations of curves with an application in neuronal data analysis, *Statist. Med.*, 2011, 30, 12, 1441-1454
- [4] DiMatteo I., Genovese C.R., Kass R.E., Bayesian curve-fitting with free-knot splines, *Biometrika*, 2001, 88, 4, 1055-1071
- [5] Kass R.E., Ventura V., Cai C., Statistical smoothing of neuronal data, *Network*, 2003, 14, 1, 5-15
- [6] Kass R.E., Ventura V., Brown E.N., Statistical issues in the analysis of neuronal data, *J. Neurophysiol.*, 2005, 94, 1, 8-25
- [7] Behseta S., Kass R.E., Testing equality of two functions using BARS, *Stat. Med.*, 2005, 24, 22, 3523-3534
- [8] Muniz-Terrera, G., Bakra, E., Hardy, R., Matthews, FE., Lunn, D., FALCon collaboration group, Modelling life course blood pressure trajectories using Bayesian adaptive splines, *Stat. Methods Med. Res.*, 2016, 25, 6, 2767-2780
- [9] Kaufman C.G., Ventura V., Kass R.E., Spline-based non-parametric regression for periodic functions and its application to directional tuning of neurons, *Stat. Med.*, 2005, 24, 14, 2255-2265
- [10] Logothetis N.K., Pauls J., Augath M., Trinath T., Oeltermann A., Neurophysiological investigation of the basis of the fMRI signal, *Nature*, 2001, 412, 6843, 150-157
- [11] Magri C., Schridde U., Murayama Y., Panzeri S., Logothetis N.K., The amplitude and timing of the BOLD signal reflects the relationship between local field potential power at different frequencies, *J. Neurosci.*, 2012, 32, 4, 1395-1407
- [12] Melloni L., Molina C., Pena M., Torres D., Singer W., Rodriguez E., Synchronization of neural activity across cortical areas correlates with conscious perception, *J. Neurosci.*, 2007, 27, 11, 2858-2865
- [13] Gao Y., Wang Q., Ding Y., Wang C., Li H., Wu X., et al., Selective Attention Enhances Beta-Band Cortical Oscillation to Speech under "Cocktail-Party" Listening Conditions, *Front. Hum. Neurosci.*, 2017, 11, 34
- [14] Neuper C., Scherer R., Wriessnegger S., Pfurtscheller G., Motor imagery and action observation: modulation of sensorimotor brain rhythms during mental control of a brain-computer interface, *Clin. Neurophysiol.*, 2009, 120, 2, 239-247
- [15] Fan J., McCandliss B.D., Fossella J., Flombaum J.I., Posner M.I., The activation of attentional networks, *Neuroimage*, 2005, 26, 2, 471-479
- [16] Neufang S., Geiger M., Homola G., Mahr M., Akhrif A., Nowak J., et al., Modulation of prefrontal functioning in attention systems by NPSR1 gene variation, *Neuroimage*, 2015, 114, 199-206
- [17] Neufang S., Akhrif A., Riedl V., Forstl H., Kurz A., Zimmer C., et al., Disconnection of frontal and parietal areas contributes to impaired attention in very early Alzheimer's Disease, *J. Alz. Dis.*, 2011, 25, 2, 309-321
- [18] Kaufman D. A., Bowers D., Okun M. S., Van Patten R., Perlstein W.M., Apathy, Novelty Processing and the P3 Potential in Parkinson's Disease, *Front. Neurol.*, 2016, 7, 95
- [19] Roh S.C., Park E.J., Shim M., Lee S.H., EEG beta and low gamma power correlates with inattention in patients with major depressive disorder, *J. Affect. Disord.*, 2016, 204, 124-130
- [20] Dosenbach N.U., Fair D.A., Cohen A.L., Schlaggar B.L., Petersen S.E., A dual-network architecture of top-down control, *Trends Cogn. Sci.*, 2008, 12, 3, 99-105
- [21] Geiger M.J., Domschke K., Homola G.A., Schulz S.M., Nowak J., Akhrif A., et al., ADORA2A genotype modulates interoceptive and exteroceptive processing in a fronto-insular network, *Eur. Neuropsychopharmacol.*, 2016, 26, 8, 1274-85
- [22] Lecrubier Y., Sheehan D.V., Weiller E., Amorim P., Bonora I., Sheehan K.H., et al., The Mini International Neuropsychiatric Interview (MINI). A short diagnostic structured interview: reliability and validity according to the CID-I, *Eur. Psychiatry*, 1997, 12, 5, 224-231
- [23] Oldfield R.C., The assessment and analysis of handedness: the Edinburgh inventory, *Neuropsychologia*, 1971, 9, 1, 97-113
- [24] Brett M., Anton J.-L., Valabregue R., Poline J.-P., Region of interest analysis using an SPM toolbox [abstract]. Presented at the 8<sup>th</sup> International Conference on Functional Mapping of the Human Brain, *Neuroimage*, 2002, 16, 497
- [25] Shimazaki H., Shinomoto S., A method for selecting the bin size of a time histogram, *Neural Comp.*, 2007, 19, 6, 1503-1527



- [26] Wallstrom G., Liebner J., Kass R.E., An Implementation of Bayesian Adaptive Regression Splines (BARS) in C with S and R Wrappers, *J. Stat. Software*, 2008, 26, 1, 1-21
- [27] Peelen M.V., Heslenfeld D.J., Theeuwes J., Endogenous and exogenous attention shifts are mediated by the same large-scale neural network, *Neuroimage*, 2004, 22, 2, 822-830
- [28] Vossel S., Thiel C.M., Fink G.R., Cue validity modulates the neural correlates of covert endogenous orienting of attention in parietal and frontal cortex, *Neuroimage*, 2006, 32, 3, 1257-1264
- [29] Shomstein S., Kravitz D.J., Behrmann M., Attentional control: temporal relationships within fronto-parietal network, *Neuropsychologia*, 2012, 50, 6, 1202-1210
- [30] Corbetta M., Shulman G.L., Control of goal-directed and stimulus-driven attention in the brain, *Nat. Rev. Neurosci.*, 2002, 3, 3, 201-215
- [31] Schechtman E., Noblejas M.I., Mizrahi A.D., Dauber O., Bergman H., Pallidal spiking activity reflects learning dynamics and predicts performance, *Proc. Natl. Acad. Sci. U S A*, 2016, 113, 41, e6281-e6289
- [32] Brown P., Williams D., Aziz T., Mazzone P., Oliviero A., Insola A., et al., Pallidal activity recorded in patients with implanted electrodes predictively correlates with eventual performance in a timing task, *Neurosci. Lett.*, 2002, 330, 2, 188-192
- [33] Ahn S., Zuber S.E., Worth R.M., Rubchinsky L.L., Synchronized beta-band oscillations in a model of the globus pallidus-subthalamic nucleus network under external input, *Front. Comput. Neurosci.*, 2016, 10-134
- [34] Muralidharan A., Jensen A.L., Connolly A., Hendrix C.M., Johnson M.D., Baker K.B., et al., Physiological changes in the pallidum in a progressive model of Parkinson's disease: are oscillations enough?, *Exp. Neurol.*, 2016, 279, 187-196.
- [35] Buzsaki G., Wang X.J., Mechanisms of gamma oscillations, *Annu. Rev. Neurosci.*, 2012, 35, 203-225
- [36] Rossi A.F., Pessoa L., Desimone R., Ungerleider L.G., The prefrontal cortex and the executive control of attention, *Exp. Brain Res.*, 2009, 192, 3, 489-497.
- [37] Fries P., Scheeringa R., Oostenveld R., Finding gamma, *Neuron*, 58, 3, 303-305
- [38] Szczepanski S.M., Crone N.E., Kuperman R.A., Auguste K.I., Parvizi J., Knight R.T., Dynamic changes in phase-amplitude coupling facilitate spatial attention in fronto-parietal cortex, *PLoS Biol.*, 2014, 12, 8, e1001936
- [39] Durston S., Davidson M.C., Tottenham N., Galvan A., Spicer J., Fossella J.A., et al., A shift from diffuse to focal cortical activity with development, *Dev. Sci.*, 2006, 9, 1, 1-8
- [40] Akhrif A., Bajer C., Wohlschläger A.M., Konrad K., Neufang S., Development-Related Dynamics in a Top-Down Control Network, *J. Neurosci. Neuroeng.*, 2013, 2, 6, 250-254
- [41] Breukelaar I.A., Antees C., Grieve S.M., Foster S.L., Gomes L., Williams L.M., et al., Cognitive control network anatomy correlates with neurocognitive behavior: A longitudinal study, *Hum. Brain. Mapp.*, 2017, 38, 2, 631-643
- [42] Reynolds J.R., Donaldson D.I., Wagner A.D., Braver T.S., Item- and task-level processes in the left inferior prefrontal cortex: positive and negative correlates of encoding, *Neuroimage*, 2004, 21, 4, 1472-1483
- [43] Buckner R.L., Koutstaal W., Functional neuroimaging studies of priming and explicit memory retrieval, *Proc. Natl. Acad. Sci. U S A*, 1998, 95, 3, 891-898
- [44] Weigl M., Mecklinger A., Rosburg T., Transcranial direct current stimulation over the left dorsolateral prefrontal cortex modulates auditory mismatch negativity, *Clin Neurophysiol.*, 2016, 127, 5, 2263-2272
- [45] Alho J., Green B.M., May P.J., Sams M., Tiitinen H., Rauschecker J.P., et al., Early-latency categorical speech sound representations in the left inferior frontal gyrus, *Neuroimage*, 2016, 129, 214-223
- [46] Li X., Gandour J., Talavage T., Wong D., Dziedzic M., Lowe M., et al., Selective attention to lexical tones recruits left dorsal frontoparietal network, *Neuroreport*, 2003, 14, 17, 2263-2266
- [47] Robbins T.W., The 5-choice serial reaction time task: behavioural pharmacology and functional neurochemistry, *Psychopharmacology*, 2002, 163, 3-4, 362-380
- [48] Voon V., Irvine M.A., Derbyshire K., Worbe Y., Lange I., Abbott S. et al., Measuring "waiting" impulsivity in substance addictions and binge eating disorder in a novel analogue of rodent serial reaction time task, *Biol. Psychiatry*, 2014, 75, 2, 148-155
- [49] Neufang S., Akhrif A., Herrmann C.G., Drepper C., Homola G.A., Nowak J., et al., Serotonergic modulation of 'waiting impulsivity' is mediated by the impulsivity phenotype in humans, *Transl. Psychiatry*, 2016, 6, 11, e940